Mesomorphous Structure Change Induced by Binding Site Difference in Ionic Complexes of Linear Polymers and Dendritic Amphiphiles

Zhiyu Cheng, Biye Ren,* Huazhong Shan, Xinxing Liu, and Zhen Tong*

Research Institute of Materials Science, South China University of Technology, Guangzhou 510640, China

Received November 30, 2007; Revised Manuscript Received January 27, 2008

ABSTRACT: Ionic complexes of linear poly(ethylenimine) (***l*PEI**) and poly(allylamine hydrochloride) (**PAH**) with 3,4,5-tris(*n*-alkan-1-yloxy)benzoic acid [**(3,4,5)*n*G1-COOH,** $n = 8, 10, 12$, where n is the number of carbon atoms in the alkyl tail) or 3,4,5-tris[(p-(*n*-dodecan-1-yloxy)benzyloxy]benzoic acid [**(4-3,4,5)12G1-COOH]** dendrons [or the corresponding potassium salts **(3,4,5)*n*G1-COOK** and **(4-3,4,5)12G1-COOK**] were prepared. The complexes were characterized with XRD, FTIR, TG, DSC, and polarized optical microscopy (POM). The complexes of ***l*PEI-(3,4,5)*n*G1** were found to be in the lamellar smectic A or C (SmA and SmC) phase, while the **PAH-(3,4,5)*n*G1** complexes were in the hexagonal columnar (Φ_h) phase. All of these complexes were in the ionic thermotropic liquid crystal state at room temperature because their melting temperature, if had, was much lower. Interestingly, the complexes ***l*PEI-(4-3,4,5)12G1** and **PAH-(4–3,4,5)12G1** were also in the same SmA or SmC phase and Φ_h phase, respectively, regardless of whether there was an additional mesogen unit benzenyloxy moiety ($-C_6H_4CH_2O-$) in the dendron, increasing the long period and adjustability of the alkyl tails. This study demonstrates that the binding site plays an important role in determining the mesomorphous structure of the polymer−dendritic amphiphile complexes. Furthermore, the **PAH** complexes exhibited a higher clear point than the corresponding ***l*PEI** complexes due to the different binding sites in these two polymers. The alkyl chain length ($n \leq 12$) of the dendron and the difference in dendron chemical structure had little effect on the mesomorphous structure and clear point of the polymer−dendritic amphiphile complexes. The present results provide a profound insight into the role of polymer topological structure in controlling the supermolecular structure for the polymer−dendritic amphiphile complexes.

1. Introduction

Polymer−amphiphile complexes based on specific noncovalent interactions, such as hydrogen bonding, charge transfer, ion binding, or coordination complexation, are attracting substantial attention in the past years due to their unique supermolecular structures and potential functions, such as low surface energy, optical and electrical devices, drug and gene delivery, etc.[1] Various nanostructures, such as lamella, rodlike, and column, have been achieved by this approach, depending on the nature of both polymers and amphiphiles, such as polar groups, alkyl side chains, and volume ratio of hydrophobic to hydrophilic moieties.[1−3] Hence, the complexation of polymers with amphiphiles promises a simple and feasible way to construct various materials with specified nanostructures and functions.

Generally, linear polymers and copolymers are most used for the complexation with amphiphiles.[1−4] Hyperbranch polymers, such as branched poly(ethylenimine) (***b*PEI**)[3] and hyperbranched polylysine (HBPL),[4a] are also used in many cases. Recently, dendrimers as a macromolecular species instead of the conventional polymer have been explored to complex with various amphiphiles for the construction of supramolecular systems with complex architectures.[4] For an example, Ujiie et al. reported ionic liquid crystal dendrimer−amphiphile complexes by the ion binding between the third generation of poly(amidoamine) (PAMAM) dendrimer and alkanoic acids (tetradecanoic, hexadecanoic, and octadecanoic acid), forming smectic A phase complexes.[5] Serrano and co-workers made a comprehensive study on the liquid crystal behavior of two series of ionic liquid crystal dendrimer−amphiphile complexes based on the ammonium salts of (PAMAM) ($G = 1-5$) and poly(propylenimine) (PPI) dendrimers ($G = 1-5$) binding with three aliphatic carboxylic acids.[6] All the complexes of PAMAM dendrimers with these carboxylic acids and most complexes of PPI dendrimers with the same carboxylic acids showed the smectic A phase, whereas the complexes of PPI ($G = 5$) exhibited square and hexagonal column mesomorphous structures with octadecanoic acid and tetradecanoic acid, respectively. Serrano et al. further investigated the ionic liquid crystal dendrimer−amphiphile complexes of the ammonium salts of PPI dendrimers ($G = 1-5$) and 4-decyloxy-, 3,4-didecyloxy-, and 3,4,5-tridecyloxybenzoic acids.[7] Interestingly, the complexes of the PPI dendrimers with 4-decyloxy- or 3,4-didecyloxybenzoic acids showed a smectic A phase, whereas the complexes of PPI with 3,4,5-tridecyloxybenzoic acid showed square and hexagonal columnar mesomorphisms. These results implied the mesomorphous structures of the complexes varying with the alkyl substitution degree of the benzoic acids. The ionic complexes of PPI dendrimers with 3-cholesteryloxycarbonylpropanoic acid reported by Tsiourvas et al. exhibited smectic C* and smectic A phases depending on dendrimer generation.[8] Analogously, Canilho et al.[4d] also found that the ionic complexes of cationic dendronized polymers and anionic sulfonated lipid surfactants menifested a thermotropic liquid crystalline behavior and nanostructures such as lamella, column rectangular, column hexagonal, and column square, depending on both the generation of dendrimers and lipid chain length.

Although macromolecular dendrimers are powerful building blocks to construct complexes with abundant supramolecular structures than conventional polymers, the synthesis of these dendrimers usually takes much more time and cost. The dendritic amphiphiles would be a better alternative for preparing the complexes of various structures and functions with linear polymers due to the facility of synthesizing dendritic amphiphiles and due to their abundant compositions and structures. Thus, use of the dendritic amphiphiles as building blocks will

* Corresponding authors: Tel (86)-20-87112886, Fax (86)-20-87110273, e-mail mcbyren@scut.edu.cn (B.R.), mcztong@scut.edu.cn (Z.T.).

10.1021/ma702664v CCC: $40.75
Published on Web 02/29/2008

Scheme 1

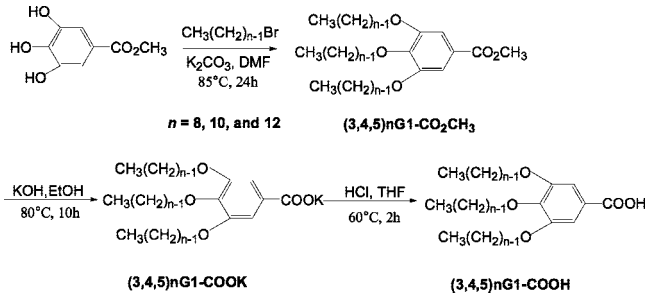

provide much more space to tune mesomorphous structures and properties for the polymer−amphiphile complexes. However, few studies on the polymer−dendritic amphiphile complexes have been reported up to date. Very recently, Beginn and co-workers prepared the ionic complex of poly(4-vinylpyridine) and mesogenic wedge-shaped sulfonic acid.[9] It was found that the complex behaved as a liquid crystal lamella phase at low degree of substitution, while a hexagonal columnar phase was observed at binding degree of 80% and higher.

The main goal of this work was to illustrate the mesomorphous phase change in the ionic complex caused by both the structure of dendritic amphiphiles and polymers. Especially the effect of the binding site position at the polymer chain and the dendritic generation as well as the alkyl tail length was investigated with X-ray diffraction (XRD), thermogravimetry (TG), differential scanning calorimetry (DSC), and polarized optical microscopy (POM). For this purpose, the complexes made of linear poly(ethylenimine) (***l*PEI**) were compared with those made of poly(allylamine hydrochloride) (**PAH**) containing the same dendritic amphiphiles because the charged amino groups loacated at backbone in ***l*PEI** and side chain in **PAH**. On the other hand, a series of trisubstituted benzoic acids dendrons with different lengths of alkyl tails were systhesized in this work with or without the benzenyloxy ($-C_6H_5CH_2O-$) spacer.

2. Experimental Section

Materials. Linear poly(ethylenimine) (***l*PEI**, Alfa, $M_w = 25\,000$ g/mol, purity 98+%), poly(allylamine hydrochloride) (**PAH**, Alfa, $M_w = 25\,000$ g/mol, purity 98+%), and methyl 3,4,5-trihydroxybenzoate (Aldrich, purity 98%) were used as received. 1-Bromooctane (purity 98%), 1-bromodecane (purity 98%), and 1-bromododecane (purity 98%) (all from Yancheng Longsheng Fine Chemical Factory, China) were distilled before use. Other reagents, such as $SOCl_2$, pyridine, Et_2O, tetrahydrofuran (THF), CH_2Cl_2, and *N,N′*-dimethylformamide (DMF), were all analysis grade chemicals and freshly distilled prior to use. The trisubstituted benzoic acid dendrons, i.e., 3,4,5-tris(*n*-alkan-1-yloxy)benzoic acid [**(3,4,5)*n*G1-COOH**, $n = 8$, 10, 12], 3,4,5-tris[(*p*-(*n*-dodecan-1-yloxy)benzyloxy]benzoic acid [**(4-3,4,5)12G1-COOH**], and their corresponding potassium salts [**(3,4,5)*n*G1-COOK** and **(4-3,4,5)12G1-COOK**] were synthesized mainly according to the method reported by Percec and co-workers[10a,b] with slight modifications (Schemes 1 and 2).

Syntheses of 3,4,5-Tris(*n*-octane-1-yloxy)benzoic Acid [(3,4,5)8G1-COOH]. First, methyl 3,4,5-tris(*n*-octane-1-yloxy)benzoate [**(3,4,5)8G1-CO_2CH_3**] was synthesized (Scheme 1). To a three-neck 100 mL round-bottom flask with a stirring bar, a mixture of 2.2 g (12.0 mmol) of methyl 3,4,5-trihydroxybenzoate and 12.5 g (90.0 mmol) of K_2CO_3 in 70 mL of DMF and 9.3 g (48.0 mmol) of 1-bromooctane were added. The mixture was heated to 85 °C under vigorous stirring under an Ar atmosphere. After about 24 h, the reaction end point was determined by TLC analysis. The reaction mixture was filtered at 50−60 °C, and the filtrate was cooled to room temperature, diluted with 100 mL of Et_2O, and transferred to a separatory funnel. The organic phase was washed three times in total with 100 mL of H_2O as 20 mL of dilute HCl, 50 mL of H_2O, and 50 mL of saturated NaCl solution. Then, the organic phase was separated, dried over $MgSO_4$, and filtered, and the solvent was evaporated. The crude product was then purified by silica gel column chromatography (eluent: petroleum ether/ethyl acetate = 10:1 in volume) to yield 5.1 g (81.6 wt %) of gold-like viscous liquid. ^{1}H NMR ($CDCl_3$, TMS, δ, ppm): 0.88 (t, 9H, $-CH_3$), 1.29 (m, 24H, $-(CH_2)_4-$), 1.47 (m, 6H, $-CH_2-CH_2-CH_2-O-$Ar), 1.79 (m, 6H, $-CH_2-CH_2-O-$Ar), 3.89 (s, 3H, $-CO_2-CH_3$), 4.01 (m, 6H, $-CH_2-O-$Ar), 7.25 (s, 2H, $-ArH-CO_2-CH_3$); $R_f = 0.68$ (eluent: petroleum ether/ethyl acetate = 10:1).

Scheme 2

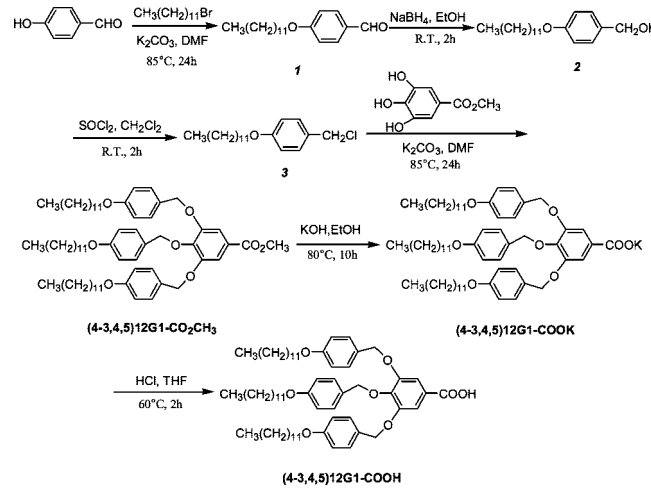

Second, **(3,4,5)8G1-CO_2CH_3** was hydrolyzed to produce **(3,4,5)8G1-COOK** and **(3,4,5)8G1-COOH.** A three-neck 100 mL round-bottom flask with a stirring bar was filled with 4.0 g (7.6 mmol) of **(3,4,5)8G1-CO_2CH_3**, 40 mL of 80% EtOH, and 4.3 g (76.0 mmol) of KOH pellets. The mixture was heated at 80 °C for about 10 h with stirring and hydrolysis was judged by TLC analysis. The reaction mixture was concentrated, and the residue was washed four times with 20 mL of H_2O, resulting in **(3,4,5)8G1-COOK**. 2.0 g (3.7 mmol) of **(3,4,5)8G1-COOK** was then transferred into a 150 mL Erlenmeyer flask and dissolved in 30 mL of THF under stirring at ca. 60 °C. The solution was acidified with dilute HCl up to pH = 1, reacted for 2 h, cooled to room temperature, and then poured into 80 mL of Et_2O. The organic phase was washed two times with 50 mL of H_2O and saturated NaCl solution, and then the organic phase was separated and dried over $MgSO_4$. After filtration and concentration, the crude product was recrystallized twice from ethanol, resulting in 1.7 g (95%) of white crystal of **(3,4,5)8G1-COOH**. ^{1}H NMR ($CDCl_3$, TMS, δ, ppm): 0.88 (t, 9H, $-CH_3$), 1.29 (m, 24H, $-(CH_2)_4-$), 1.47 (m, 6H, $-CH_2-CH_2-CH_2-O-$Ar), 1.79 (m, 6H, $-CH_2-CH_2-O-$Ar), 4.02 (m, 6H, $-CH_2-O-$Ar), 7.32 (s, 2H, $-ArH_2-CO_2H$). Anal. Calcd for $C_{31}H_{54}O_5$: C, 73.47; H, 10.74. Found: C, 73.29; H, 10.70.

3,4,5-Tris(*n*-decane-1-yloxy)benzoic acid, **(3,4,5)10G1-COOH**, and 3,4,5-tris(*n*-dodecan-1-yloxy)benzoic acid, **(3,4,5)12G1-COOH**, were synthesized following a similar procedure to that for **(3,4,5)8G1-COOH**. For **(3,4,5)10G1-COOH**: ^{1}H NMR ($CDCl_3$, TMS, δ, ppm) 0.88 (t, 9H, $-CH_3$), 1.29 (m, 36H, $-(CH_2)_6-$), 1.47 (m, 6H, $-CH_2-CH_2-CH_2-O-$Ar), 1.77 (m, 6H, $-CH_2-CH_2-O-$Ar), 4.02 (m, 6H, $-CH_2-O-$Ar), 7.34 (s, 2H, ArH_2-CO_2H). Anal. Calcd for $C_{37}H_{66}O_5$: C, 75.20; H, 11.26. Found: C, 75.42; H, 11.23. For **(3,4,5)12G1-COOH**: ^{1}H NMR ($CDCl_3$, TMS, δ, ppm): 0.88 (t, 9H, $-CH_3$), 1.28 (m, 48H, $-(CH_2)_8-$), 1.47 (m, 6H, $-CH_2-CH_2-CH_2-O-$Ar), 1.79 (m, 6H, $-CH_2-CH_2-O-$Ar), 4.02 (m, 6H, $-CH_2-O-$Ar), 7.32 (s, 2H, $-ArH_2-CO_2H$). Anal. Calcd for $C_{43}H_{78}O_5$: C, 76.50; H, 11.65. Found: C, 76.54; H, 11.72.

Syntheses of 3,4,5-Tri[*p*-(*n*-dodecan-1-yloxy)benzyloxy]benzonic Acid [(4–3,4,5)12G1-COOH] and [(4-3,4,5)12G1-COOK]. **(4–3,4,5)12G1-COOH** was synthesized according to the procedure reported by Percec and co-workers (Scheme 2).[10c] ^{1}H NMR ($CDCl_3$,

Scheme 3

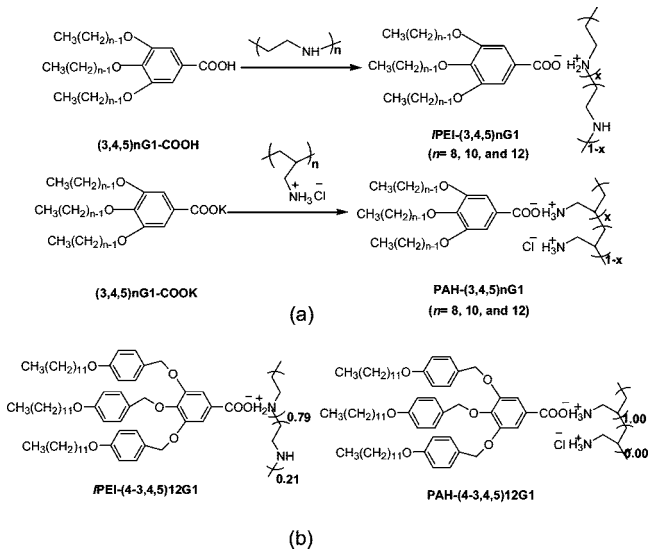

TMS, δ, ppm): 0.88 (t, 9H, $-CH_3$), 1.28 (m, 48H, $-(CH_2)_8-$), 1.47 (m, 6H, $-CH_2-CH_2-CH_2-O-Ar$), 1.79 (m, 6H, $-CH_2-CH_2-O-Ar$), 3.96 (two overlapped t, 6H, $-CH_2-O-Ar$), 5.02 (s, 2H, $-CH_2-O-Ar-COOH$ from para position of benzoic group), 5.05 (s, 4H, $-CH_2-O-Ar-COOH$ from 3- and 5 -positions of benzoic group), 6.77 (d, 2H, $-O-Ar-H-CH_2-O-Ar-COOH$ from 3- and 5-positions of center benzylic unit), 6.91 (d, 4H, $-O-Ar-H-CH_2-O-Ar-COOH$ from 3- and 5-positions of external benzylic units), 7.28 (d, 2H, $-O-Ar-H-CH_2-O-Ar-COOH$ from the 2- and 6-positions of the internal benzylic unit), 7.34 (d, 4H, $-O-Ar-H-CH_2-O-Ar-COOH$ from 2- and 6-positions of the external benzylic units), 7.45 (s, 2H, $-Ar-H-COOH$ from the 2- and 6-positions). IR (KBr plate): 1670 cm^{-1} ($\nu_{-C=O}$). Anal. Calcd for $C_{64}H_{96}O_8$: C, 77.37; H, 9.74. Found: C, 77.42; H, 10.09.

Complex Preparation. The ***l*PEI** complexes ***l*PEI-(3,4,5)nG1** and ***l*PEI-(4–3,4,5)12G1** were respectively prepared by mixing 3,4,5-tris(*n*-alkan-1-yloxy)benzoic acid, [**(3,4,5)*n*G1-COOH**, n = 8, 10, 12], and 3,4,5-tris[(*p*-(*n*-dodecan-1-yloxy)benzyloxy]benzoic acid, [**(4-3,4,5)12G1-COOH**], dendrons with ***l*PEI** in ethanol solution at about 75 °C just below its boiling temperature under reflux (Scheme 3). A general procedure was as follows: 1 mmol of dendron was dissolved in 20 mL of ethanol at about 75 °C and slowly added dropwise into the 1:1 stoichiometric ***l*PEI** ethanol solution under stirring for 5 h. The solvent was slowly vaporized until white solid appeared. The resulting solid complex was separated by filtration, washed with hot ethanol, and then dried under vacuum for 48 h at room temperature.

The PAH complexes **PAH-(3,4,5)*n*G1** and **PAH-(4-3,4,5)12G1** were prepared by respectively mixing the potassium salt of 3,4,5-tris(*n*-alkan-1-yloxy)benzoic acid [**(3,4,5)*n*G1-COOK**, n = 8, 10, 12] and 3,4,5-tris[(*p*-(*n*-dodecan-1-yloxy)benzyloxy]benzoic acid [**(4-3,4,5)12G1-COOK**] dendrons with PAH in 90% ethanol/H_2O solution at about 75 °C (Scheme 3). As a general procedure, 1 mmol of dendron was dissolved in 20 mL of 90% ethanol aqueous solution at about 75 °C and slowly added dropwise into 90% ethanol/water mixture containing a 1:1 stoichiometric PAH under stirring. A white solid appeared in the mixture. Then the mixture was cooled to room temperature and filtered. The precipitate was washed with hot water and ethanol and then dried under vacuum for 48 h at room temperature.

For preparing complex films, a THF solution of the complex of 30 g/L was coated on a quartz glass at room temperature and dried under vacuum at 40 °C for 24 h.

Measurements. Fourier transform infrared (FTIR) spectra of the complexes were recorded on a Bruker Vector 33 FTIR spectrometer using KBr pellets at room temperature. X-ray diffraction (XRD) of the complex powder was performed in transmission geometry with an X'pert PRO diffractometer (40 kV and 40 mA) using Cu Kα radiation (wavelength $\lambda = 0.154$ nm) at room temperature. The 2θ ranged from 1° to 30°, and the scan step was 0.01° in 2θ with a counting time of 1 s/step. The differential scanning calorimetry (DSC) experiment was carried out with 3–5 mg of sample in a 6 mm aluminum pan on a Netzsch DSC 204 under a nitrogen atmosphere at heating or cooling rate of 10 °C/min following the temperature sequence as room temperature → 140 °C → −60 °C → 140 °C for the ***l*PEI** series complexes and room temperature → 220 °C → −60 °C → 220 °C for the PAH series complexes, respectively. Thermogravimetry (TG) was measured with a Netzsch TG 209 under a nitrogen atmosphere at heating rate of 10 °C/min starting from room temperature to 800 °C. The C, H, and N contents (wt %) of the complex were determined with a Vario EL elemental analyzer. ^1H NMR spectra were recorded on a Varian INOVA 500NB spectrometer. A polarized optical microscope (POM) of Zeiss Axiophot was used with a Linkam hot stage. The sample was heated from room temperature to 140 °C for the ***l*PEI** series complexes or 220 °C for the PAH series complexes and held for 3 min to remove the heat history, then cooled to room temperature, and subsequently heated again to 80 °C at the rate of 10 °C/min. The POM photos were taken at 80 °C for ***l*PEI** series and 160 °C for PAH series complexes.

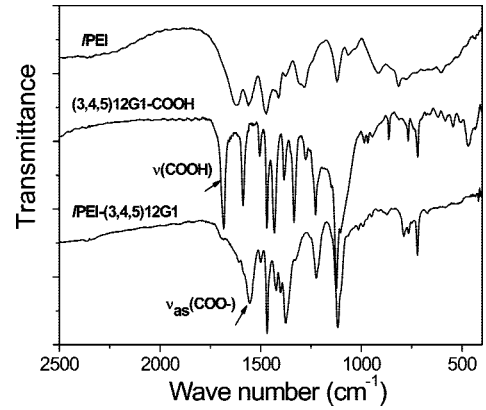

Figure 1. FT-IR spectra of the ***l*PEI**, **(3,4,5)12G1COOH**, and ***l*PEI-(3,4,5)12G1** complex. The curves were vertically shifted to avoid overlapping.

3. Results and Discussion

Complex Formation. The formation of ionic complexes of ***l*PEI** or PAH with **(3,4,5)*n*G1-COOH** or **(4-3,4,5)12G1-COOH** (or their potassium salts) was observed as white precipitates during mixing. The ***l*PEI** series complexes were also observed with FT-IR spectra as shown in Figure 1 for ***l*PEI**, **(3,4,5)12G1-COOH**, and ***l*PEI-(3,4,5)12G1** complex for examples. The strong absorption band at ca. 1552–1557 cm^{-1} corresponded to the asymmetric stretching of the carboxylate groups of dendrons, and the carbonyl stretching band at about 1682–1687 cm^{-1} disappeared. A weak absorption band appearing at ca. 1610 cm^{-1} is assigned to deformation vibration of the H_3N^+- or $-H_2N^+-$ groups, indicating the presence of protonated amino groups.

The composition of the ionic complex χ, as the mole ratio of carboxyl to amino groups, was estimated on N content determined by elemental analysis and listed in Table 1. As known from the χ values of 0.79−1.0 with reasonable error, the composition of the complexes approached to a 1:1 stoichiometry in respect to the ionic groups, suggesting that the dendrons had a strong binding capability to the polymer chains. The deviation from the 1:1 stoichiometry seems to be resulted from the steric hindrance due to the larger volume of the bound dendritic amphiphiles.

Mesomorphous Structure of lPEI-(3,4,5)*n*G1 and PAH-(3,4,5)*n*G1 Complexes. XRD measurements were performed to reveal mesomorphous structure of the complexes. Figures 2

Table 1. Composition and Thermal Properties of the Complexes lPEI-(3,4,5)*n*G1, lPEI-(4-3,4,5)12G1, PAH-(3,4,5)*n*G1, and PAH-(4–3,4,5)12G1 (*n* = 8, 10, 12)

complex	*N* (wt %)	χ	T_m[a] (°C)	ΔH_m[b] (J/g)	T_g (°C)	T_i[a] (°C)	ΔH_i[b] (J/g)	T_d (°C)
***l*PEI-(3,4,5)8G1**	2.55	1.00				102	1.06	384
***l*PEI-(3,4,5)10G1**	2.26	0.98				103	0.96	402
***l*PEI-(3,4,5)12G1**	2.20	0.88	8	16.47		111	1.04	406
***l*PEI-(4-3,4,5)12G1**	1.60	0.79	−13	13.58		153	0.74	398
PAH-(3,4,5)8G1	2.78	0.88			79	189	1.54	415
PAH-(3,4,5)10G1	2.42	0.87			79	192	1.32	427
PAH-(3,4,5)12G1	1.93	0.99	−11	21.79	83	197	1.43	428
PAH-(4-3,4,5)12G1	1.35	1.00	−12	16.41	92	211	2.04	395

[a] DSC peak value. [b] Melting heat at the second heating run.

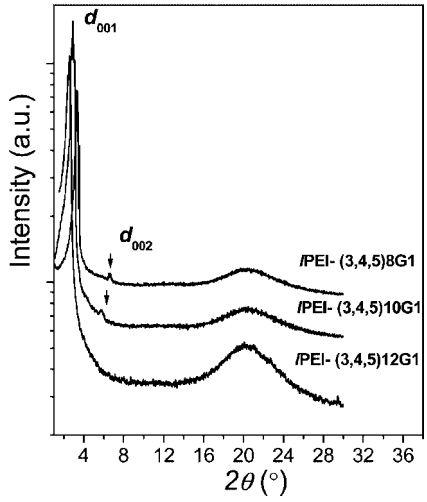

Figure 2. XRD patterns of the ***l*PEI-(3,4,5)*n*G1** (*n* = 8, 10, and 12) complexes at room temperature.

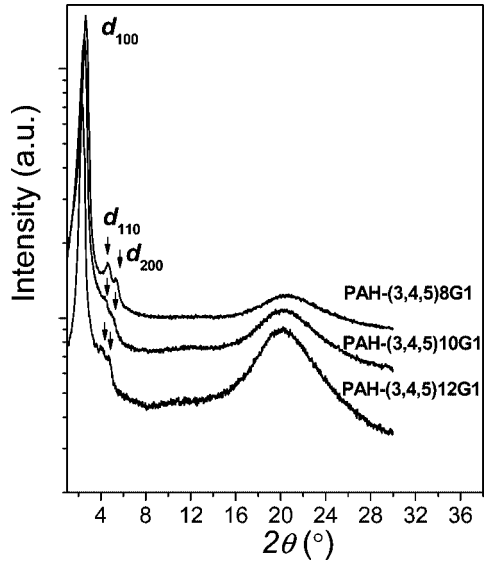

Figure 3. XRD patterns of the **PAH-(3,4,5)nG1** (*n* = 8, 10, and 12) complexes at room temperature.

and 3 illustrate the XRD patterns at room temperature for the ***l*PEI-(3,4,5)*n*G1** and **PAH-(3,4,5)*n*G1** complexes, respectively. In the wide-angle range, only one broad peak appears at $2\theta \approx 20°$ corresponding to the distance between the conformationally disordered alkyl chains. This indicates noncrystalline structure in these solid complexes at room temperature. In the small-angle range, there are several reflection peaks, suggesting the existence of mesomorphous structures in the complexes at room temperature.

For the ***l*PEI-(3,4,5)*n*G1** complexes in Figure 2, one or two reflections at the equidistant position in d^{-1} scale as 1:2 implies

Table 2. X-ray Data for the Complexes *l*PEI-(3,4,5)*n*G1 (*n* = 8, 10, 12), and *l*PEI-(4-3,4,5)12G1 at Room Temperature

complexes	d_{001} (Å)	d_{002} (Å)	mesophases
***l*PEI-(3,4,5)8G1**	27.0	13.4	lamellar
***l*PEI-(3,4,5)10G1**	30.2	15.1	lamellar
***l*PEI-(3,4,5)12G1**	34.6		lamellar
***l*PEI-(4-3,4,5)12G1**	41.3	20.6	lamellar

the lamella smectic A or smectic C (SmA or SmC) mesomorphous structure existing in these complexes.[7] As expected, the corresponding long period increases with *n* (Table 2). Normally, surfactants are organized in two different ways in the polymer−surfactant complex as bilayer with opposite chain ends and monolayer with interdigitated alkyl tails.[1d,f] We take the **(3,4,5)8G1-COOH** as an example to estimate total length of the dendrons. The increment of one carbon atom in a stretched alkyl chain is about 1.25 Å, and the length of a phenoxy moiety (C_6H_5−O) is about 5.3 Å.[7] Therefore, the length of **(3,4,5)8G1-COOH** should be about 15.3 Å. This value is slightly larger than a half of the long period of the ***l*PEI-(3,4,5)8G1** complex (13.5 Å). Usually, the alky tails take somewhat coiled conformation not completely stretched and ordered arrangement in the complex as judged from the XRD profiles in wide-angle range. This implies that the actual length of **(3,4,5)8G1-COOH** in the complex should be shorter than 15.3 Å. Therefore, we consider that bound dendrons in the complexes are stacked into a bilayer arrangement.

In our previous study, we reported that the branching of polymer backbone significantly altered the crystal and mesomorphous structures of the complex made of linear or branching PEI and long-chain aliphatic acid of octadecanoic acid.[3] Recently, Serrano and co-workers also demonstrated that the chemical structure and generation number of dendrimers led to different mesomorphism for the ionic complexes of dendrimers and long-chain alkanoic acids.[6] Hence, in order to reveal the backbone effect on the complex mesomorphous structure, we further studied the **PAH-(3,4,5)*n*G1** complexes, where the binding sites were at side chains in PAH but at backbone in linear PEI. For the **PAH-(3,4,5)*n*G1** complexes, the XRD profiles in small-angle range in Figure 3 exhibit reflections different from those for the ***l*PEI-(3,4,5)*n*G1** complexes. Three reflections were observed at the ratio of $d_{100}^{-1}:d_{110}^{-1}:d_{200}^{-1} = 1:\sqrt{3}:2$, indicating a hexagonal columnar mesophase (Φ_h). Similar results have been reported by Percec et al.[11] Moreover, these **PAH-(3,4,5)*n*G1** complexes behave birefringent texture different from that of the ***l*PEI-(3,4,5)*n*G1** complexes under POM at room temperature. For the hexagonal phase, the lattice parameter *a* can be calculated from the *q* value corresponding to the reflection of (*hkl*) as[4a]

$$a = \frac{4\pi}{q\sqrt{3}}\sqrt{(h^2 + hk + k^2)} \quad (1)$$

The measured d_{hkl} ($= 2\pi/q$) value and lattice parameter so calculated for the **PAH-(3,4,5)*n*G1** complexes in the hexagonal columnar phase are listed in Table 3. Taking **PAH-(3,4,5)8G1** as an example (e.g., $d_{100} = 33.3$ Å, $d_{110} = 19.2$ Å, $d_{200} = 16.6$

Table 3. X-ray Data for the Complexes PAH-(3,4,5)*n*G1 (n = 8, 10, 12) and PAH-(4-3,4,5)12G1 at Room Temperature

complexes	d_{100} (Å)	d_{110} (Å)	d_{200} (Å)	mesophase	d_{100}[a] (Å)	a[b] (Å)
PAH-(3,4,5)8G1	33.3	19.2	16.6	hexagonal	33.2	38.3
PAH-(3,4,5)10G1	35.0	20.0	17.3	hexagonal	34.7	40.1
PAH-(3,4,5)12G1	37.2	21.5	18.5	hexagonal	37.1	42.8
PAH-(4-3,4,5)12G1	43.2	24.5	21.6	hexagonal	42.9	49.5

[a] $\langle d_{100}\rangle = (d_{100} + \sqrt{3}d_{110} + 2d_{200})/3$. [b] $a = 2\langle d_{100}\rangle/\sqrt{3}$.

Å), the lattice parameter a is 38.3 Å, which is much larger than the twice of total length of the bound dendron **(3,4,5)8G1-COOK** (ca. 30.6 Å). It is worth noting from Table 3 that the lattice parameter a increases with increasing length of the dendron alkyl tails. This means that the column was formed with a PAH core surrounded by bound dendrons and stacked in a loose hexagonal form. Recently, Canilho et al. demonstrated that the comblike supramolecular dendronized polymer−surfactant complexes formed columnar and lamellar nanostructures, depending on generations of the dendronized polymers and alkyl chain length of the surfactants.[4b,c] A transition from columnar to lamellar mesomorphous stack was observed with decreasing the volume ratio of dendrons to surfactants. For their complexes in the columnar phase, the dendrons pack in the continuous phase, and the attached surfactants pack in the cylinders due to larger volume ratio of dendrons to surfactants. In the percent work, the linear polymer PAH forms the core of the cylindrical phase, and the bound dendrons form the continuous phase because the bound dendrons have a much larger volume than PAH.

In order to understand the nature of these mesomorphous structures in the ***l*PEI-(3,4,5)*n*G1** and **PAH-(3,4,5)*n*G1** complexes, we determined their thermal properties with TG and DSC. The TG shows that there is no significant weight loss up to 220 °C for these complexes (data are not shown here). The temperature of maximum weight-loss rate T_d in Table 1 is higher for the **PAH-(3,4,5)*n*G1** complexes than that for the ***l*PEI-(3,4,5)*n*G1** complexes. All the complexes exhibit a higher thermal stability than the corresponding pure dendrons and polymers, and T_d increases with increasing aliphatic chain length of the dendrons as n from 8 to 12. The enhanced thermal stability should be attributed to the strong ionic interaction between the polymers and dendrons, as previously reported for the complexes based on PEI and alkanoic acids.[3]

For the ***l*PEI-(3,4,5)*n*G1** and **PAH-(3,4,5)*n*G1** complexes with n = 8 and 10, no melting transition was observed from the DSC trace above −60 °C, but a melting point T_m was determined for the ***l*PEI-(3,4,5)12G1** and **PAH-(3,4,5)12G1** as 8 and −11 °C (Table 1), respectively, due to the melting of the dendron alkyl chain crystal. This fact implies that there should be no crystalline phase in the complexes at room temperature owing to the short alkyl chains and a centered phenoxy moiety in the dendrons. What interesting is that there exists a weak endothermic peak in each heating curve between 102 and 111 °C for the ***l*PEI-(3,4,5)*n*G1** complexes and between 189 and 197 °C for the **PAH-(3,4,5)*n*G1** complexes. Combining with the finding from XRD in Figures 2 and 3, we consider that these complexes are in the liquid crystal state at room temperature, and the weak endothermic transition T_i corresponds to the transition from liquid crystal to isotropic phase. As seen from Table 1, T_i of the ***l*PEI-(3,4,5)*n*G1** and **PAH-(3,4,5)*n*G1** complexes increases slightly with increasing n, indicating that the alkyl chain length of the dendrons has no significant effect on T_i. But the T_i for the **PAH-(3,4,5)*n*G1** complexes (from 189 to 197 °C) is much higher than that for the ***l*PEI-(3,4,5)*n*G1** complexes (from 102 to 111 °C). The reason for this is still unknown.

It is therefore important to directly observe the liquid crystal phase in the complexes with POM. Figure 4 illustrates POM photographs of the complexes taken at 80 °C. As expected, the birefringent random polygon-like texture was observed under POM above room temperature for these complexes. This birefringence only appears at temperatures between T_m and T_i and disappears when temperature is above T_i (Figure 5). Therefore, the ***l*PEI-(3,4,5)*n*G1** and **PAH-(3,4,5)*n*G1** complexes are found in the liquid crystalline state of ionic thermotropic SmA (or SmC) and hexagonal columnar phases between room temperature and T_i.

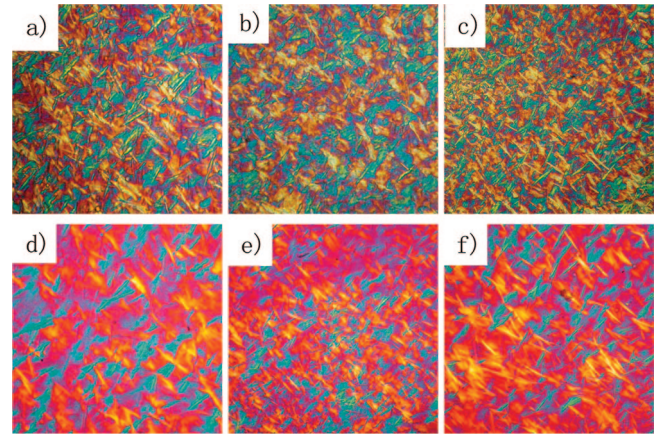

Figure 4. Polarized optical micrographs taken at 80 °C for the complexes: (a) ***l*PEI-(3,4,5)8G1**; (b) ***l*PEI-(3,4,5)10G1**; (c) ***l*PEI-(3,4,5)12G1**; (d) **PAH-(3,4,5)8G1**; (e) **PAH-(3,4,5)10G1**; (f) **PAH-(3,4,5)12G1**.

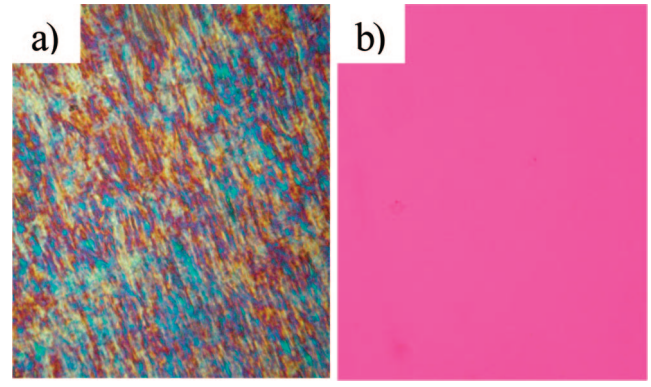

Figure 5. Polarized optical micrographs for the complex ***l*PEI-(3,4,5)12G1**: (a) 80 °C after shearing; (b) 115 °C above T_i.

The above results seem to suggest that the same amphiphilic dendron induces different mesomorphous structures of liquid crystal when forming the ionic complex with polyelectrolytes, e.g., the lamellar SmA or SmC phase for the ***l*PEI-(3,4,5)*n*G1** and the hexagonal columnar Φ_h phase for the **PAH-(3,4,5)*n*G1** complexes. Thus, the location of binding sites at the polymer chain plays a key role to determine the mesomorphous structure when the dendrons have short alkyl tails as $n \leq 12$ because the amino groups are at backbone for ***l*PEI** and at side chain for **PAH**. Figure 6 shows the stacking model for the complexes at room temperature: lamella phase for *l*PEI-containing complexes and hexagonal column phase for PAH-containing complexes.

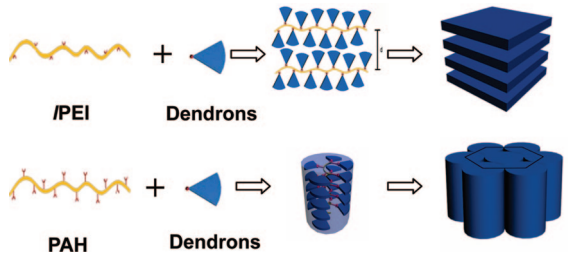

Figure 6. Stacking models for the complexes at room temperature: lamella phase for ***l*PEI** series complexes and hexagonal column phase for **PAH** series complexes.

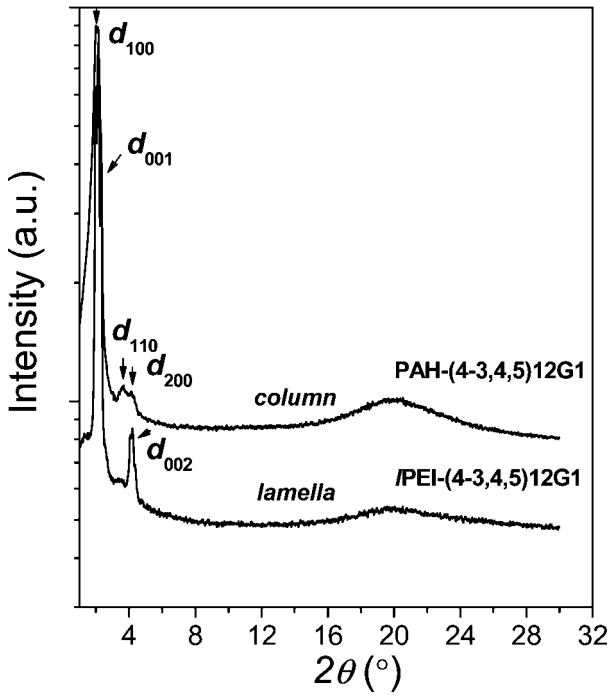

Figure 7. XRD patterns of the ***l*PEI-(4-3,4,5)12G1** and **PAH-(4-3,4,5)12G1** complexes at room temperature.

Comparison of *l*PEI-(4-3,4,5)12G1 and PAH-(4-3,4,5)-12G1 Complexes. As discussed above, different binding locations at the polymer chain cause different liquid crystalline phases for the polyelectrolyte−amphiphilic dendron complex. We were still interested in whether the dendron structure affected the complex structure, so the ionic complexes of ***l*PEI** and **PAH** with **(4–3,4,5)12G1-COOH** or **(4-3,4,5)12G1-COOK** dendron were investigated. Figure 7 depicts the XRD patterns of the ***l*PEI-(4-3,4,5)12G1** and **PAH-(4–3,4,5)12G1** complexes at room temperature. In the wide-angle range, the broad diffraction peak at $2\theta \approx 20°$ indicates their amorphous structure at room temperature. This is also understood from their melting point of ca. −13 and −12 °C (Table 1). While in the small-angle range, some characteristic reflections suggest some mesomorphous structure in these complexes. For the ***l*PEI-(4-3,4,5)12G1**, two reflections appeared at the equidistant positions in d^{-1} scale as 1:2 (e.g., $d_{001} = 41.3$ Å and $d_{002} = 20.6$ Å), implying a lamella SmA or SmC stacking. The long period d_{001} increases when compared with that of 34.6 Å for the corresponding ***l*PEI-(3,4,5)12G1** complex (Table 2). The presence of a benzenyloxy moiety ($-C_6H_5CH_2O-$) in the dendrons tends to increase the long period. In contrast, the XRD pattern for the **PAH-(4-3,4,5)12G1** complex shows amorphous structure and three reflections at position of $d_{100}^{-1}:d_{110}^{-1}:d_{200}^{-1} = 1:\sqrt{3}:2$ ($d_{100} = 43.2$ Å, $d_{110} = 24.5$ Å, and $d_{200} = 21.6$ Å) at room temperature (Figure 7 and Table 3). This implies a hexagonal column mesomorphous (Φ_h) phase similar to that in the **PAH-(3,4,5)12G1** complexes. The lattice parameter a was estimated as 49.5 Å due to the increase in the dendron size.

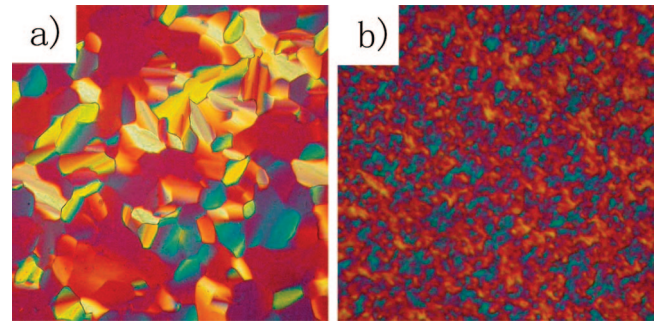

Figure 8. Polarized optical micrographs taken at 160 °C for the complexes: (a) ***l*PEI-(4-3,4,5)12G1**; (b) **PAH-(4-3,4,5)12G1**.

T_m and T_i are listed in Table 1 for these two complexes. It is worth noting that the ***l*PEI-(4-3,4,5)12G1** complex has much lower T_i (153 °C) than that of the **PAH-(4-3,4,5)12G1** complex (211 °C). POM photographs in Figure 8 illustrate the evident birefringent random polygon-like texture for the ***l*PEI-(4-3,4,5)12G1** complex similar to the ***l*PEI-(3,4,5)12G1** complex. It should be mentioned that the oriented texture was also observed after being sheared in one direction between T_m and T_i, and the birefringence disappeared when the temperature was above T_i. Consequently, the ***l*PEI-(4-3,4,5)12G1** complex is also in the same lamella SmA or SmC liquid crystalline phase at room temperature as the ***l*PEI-(3,4,5)*n*G1** complexes.

A similar birefringent texture was observed under polarized light between T_m and T_i (Table 1) for the **PAH-(4-3,4,5)12G1** complex (Figure 8), which was oriented if being sheared. Hence, the **PAH-(4-3,4,5)12G1** complex forms the hexagonal Φ_h liquid crystalline phase at room temperature. The above facts also support our opinion that the mesomorphous structure of the polyelectrolyte−amphiphilic dendron complex is determined mainly by the location of binding sites on the polymer chain, which also changes the clear point T_i substantially.

4. Conclusions

In conclusion, the polymer−amphiphilic dendron complexes prepared through the ionic binding of trisubstituted benzoic acid dendrons on linear poly(ethylenimine) or poly(allylamine hydrochloride) exhibit two mesomorphous structures: lamella for the ***l*PEI** series and hexagonal column for the **PAH** series complexes irrespective of the chemical structure and alkyl tail length ($n \leq 12$) of the dendrons. This research demonstrates that the binding sites play an important role in determining the mesomorphous structure for the polymer−dendritic amphiphile complexes. The present results also provide profound insights into the role of the topological structure of polymers in the formation of various supermolecular structures in polymer−amphiphile complexes.

Acknowledgment. The financial support from the NSF of China (50673029 and 20534020), NCET, and the NSF of Guangdong Province (05006561) is gratefully acknowledged.

References and Notes

(1) (a) Zhou, S.; Chu, B. *Adv. Mater.* **2000**, *12*, 545. (b) Antonietti, M.; Conrad, J.; Thünemann, A. F. *Macromolarcules* **1994**, *27*, 6007. (c) Faul, C. F. C.; Antonietti, M. *Adv. Mater.* **2003**, *15*, 673. (d) Thünemann, A. F. *Prog. Polym. Sci.* **2002**, *27*, 1473. (e) Thünemann, A. F.; Ruppelt, D.; Schnablegger, H.; Blaul, J. *Macromolecules* **2000**, *33*, 2124. (f) Thünemann, A. F.; General, S. *Langmuir* **2000**, *16*, 9634. (g) Thünemann, A. F. *Langmuir* **2000**, *16*, 824. (h) Ujiie, S.; Takagi, S.; Sato, M. *High Perform. Polym.* **1998**, *10*, 139. (i) Macknight, W. J.; Ponomarenko, E. A.; Tirrell, D. A. *Acc. Chem. Res.* **1998**, *31*, 781.

(j) Zhou, S.; Zhao, Y.; Cai, Y.; Wang, D.; Xu, D. *Chem. Commun.* **2003**, 1932. (k) Ober, C. K.; Wegner, G. *Adv. Mater.* **1997**, *9*, 17. (l) Chen, L.; Xu, S.; McBranch, D.; Whitten, D. *J. Am. Chem. Soc.* **2000**, *122*, 9302.

(2) (a) Ikkala, O.; Brinke, G. T. *Science* **2002**, *292*, 2407. (b) Ikkala, O.; Brinke, G. T. *Chem. Commun.* **2004**, 2131.

(3) (a) Ren, B.; Cheng, Z.; Tong, Z.; Liu, X.; Wang, C.; Zeng, F. *Maromolecules* **2005**, *38*, 5675. (b) Ren, B.; Cheng, Z.; Tong, Z.; Liu, X.; Wang, C.; Zeng, F. *Macromolecules* **2006**, *39*, 6552. (c) Cheng, Z.; Ren, B.; Gao, M.; Liu, X.; Tong, Z. *Macromolecules* **2007**, *40*, 7638. (d) Ren, B.; Tong, Z.; Liu, X.; Wang, C.; Zeng, F. *Langmuir* **2004**, *20*, 10737.

(4) (a) Caniho, N.; Scholl, M.; Klok, H. A.; Mezzenga, R. *Macromolecules* **2007**, *40*, 8374. (b) Canilho, N.; Kasemi, E.; Schlüter, A. D.; Mezzenga, R. *Macromolecules* **2007**, *40*, 2822. (c) Canilho, N.; Kasemi, E.; Schlüter, A. D.; Ruokolainen, J.; Mezzenga, R. *Macromolecules* **2007**, *40*, 7609. (d) Zhang, A.; Zhang, B.; Wächtersbach, E.; Schmidt, M.; Schlüter, A. D. *Chem.—Eur. J.* **2003**, *9*, 6083. (e) Zhang, A.; Okrasa, L.; Pakula, T.; Schlüter, A. D. *J. Am. Chem. Soc.* **2004**, *126*, 6658. (f) Kasëmi, E.; Zhuang, W.; Rabe, J. P.; Fischer, K.; Schmidt, M.; Colussi, M.; Keul, H.; Yi, D.; Colfen, H.; Schlüter, A. D. *J. Am. Chem. Soc.* **2006**, *128*, 5091.

(5) (a) Ujiie, S.; Yano, Y.; Mori, A. *Mol. Cryst. Liq. Cryst.* **2004**, *411*, 483. (b) Binnemans, K. *Chem. Rev.* **2005**, *105*, 4148.

(6) Martín-Rapún, R.; Marcos, M.; Omenat, A.; Barberá, J.; Romero, P.; Serrano, J. L. *J. Am. Chem. Soc.* **2005**, *127*, 7397.

(7) Marcos, M.; Martín-Rapún, R.; Omenat, A.; Barberá, J.; Serrano, J. L. *Chem. Mater.* **2006**, *18*, 1206.

(8) Tsiourvas, D.; Felekis, T.; Sideratou, Z.; Paleos, C. M. *Liq. Cryst.* **2004**, *31*, 739.

(9) Zhu, X.; Beginn, U.; Moller, M.; Gearba, R. I.; Anokhin, D. V.; Ivanov, D. A. *J. Am. Chem. Soc.* **2006**, *128*, 16928.

(10) (a) Percec, V.; Holerca, M. N.; Uchida, S.; Cho, W.; Ungar, G.; Lee, Y.; Yeardley, D. J. P. *Chem.—Eur. J.* **2002**, *8*, 1106. (b) Percec, V.; Schlueter, D.; Ronda, J. C.; Johansson, G.; Ungar, G.; Zhou, J. P. *Macromolecules* **1996**, *29*, 1464. (c) Percec, V.; Heck, J. *J. Polym. Sci., Part A: Polym. Chem.* **1991**, *29*, 591. (d) Percec, V.; Johansson, G.; Heck, J.; Ungar, G.; Batty, S. V. *J. Chem. Soc., Perkin Trans. 1* **1993**, 1411. (e) Percec, V.; Cho, W.-D.; Ungar, G. *J. Am. Chem. Soc.* **2000**, *122*, 10273. (f) Percec, V.; Cho, W.-D.; Ungar, G.; Yeardley, D. J. P. *J. Am. Chem. Soc.* **2001**, *123*, 1302.

(11) Percec, V.; Glodde, M.; Bera, T. K.; Miura, Y.; Shiyanovskaya, I.; Singer, K. D.; Balagurusamy, V. S. K.; Heiney, P. A.; Schnell, I.; Rapp, A.; Spiess, H. W.; Hudson, S. D.; Duan, H. *Nature (London)* **2002**, *419*, 384.

MA702664V